Neuron
Article

GDE2 Regulates Subtype-Specific Motor Neuron Generation through Inhibition of Notch Signaling

Priyanka Sabharwal,[1] Changhee Lee,[1] Sungjin Park,[1] Meenakshi Rao,[1,2] and Shanthini Sockanathan[1,*]
[1]The Solomon Snyder Department of Neuroscience, The Johns Hopkins University School of Medicine, PCTB1004, 725 N. Wolfe Street, Baltimore, MD 21205, USA
[2]Present address: Department of Pediatrics, Children's Hospital Boston, 300 Longwood Avenue, Boston, MA 02115, USA
*Correspondence: ssockan1@jhmi.edu
DOI 10.1016/j.neuron.2011.07.028

SUMMARY

The specification of spinal interneuron and motor neuron identities initiates within progenitor cells, while motor neuron subtype diversification is regulated by hierarchical transcriptional programs implemented postmitotically. Here we find that mice lacking GDE2, a six-transmembrane protein that triggers motor neuron generation, exhibit selective losses of distinct motor neuron subtypes, specifically in defined subsets of limb-innervating motor pools that correlate with the loss of force-generating alpha motor neurons. Mechanistically, GDE2 is expressed by postmitotic motor neurons but utilizes extracellular glycerophosphodiester phosphodiesterase activity to induce motor neuron generation by inhibiting Notch signaling in neighboring motor neuron progenitors. Thus, neuronal GDE2 controls motor neuron subtype diversity through a non-cell-autonomous feedback mechanism that directly regulates progenitor cell differentiation, implying that subtype specification initiates within motor neuron progenitor populations prior to their differentiation into postmitotic motor neurons.

INTRODUCTION

The mechanisms that control neuronal diversity are complex and involve a constant interplay between extrinsic signaling pathways and intrinsic cell-autonomous molecular networks (reviewed in Dasen and Jessell, 2009; Dehay and Kennedy, 2007). These processes operate at different stages of the cell cycle according to cellular context such that neuronal fate can be specified within the last cell division cycle of progenitors or within postmitotic neurons themselves. While the events that govern and distinguish the identities of distinct neuronal classes are beginning to be understood, the mechanisms that impose subtype diversity within a single class of neurons are not as clear.

One system in which this question has been extensively studied is in developing spinal motor neurons (Dasen and Jessell, 2009). The complexity and range of motor behaviors require the coordinate activation of multiple muscle groups, each of which is innervated by specific groups of motor neurons. Individual motor neuron groups are highly organized in terms of their cell body distribution, projection patterns, and function and consist of force-generating alpha motor neurons that innervate extrafusal muscle fibers and stretch-sensitive gamma motor neurons that innervate intrafusal muscle fibers of the muscle spindles (Dasen and Jessell, 2009; reviewed in Kanning et al., 2010). The integration of input from both alpha and gamma motor neurons is essential for coordinated motor movement to occur (Kanning et al., 2010).

How is diversity engendered in developing motor neurons? All motor neurons initially derive from ventral progenitor cells that are specified to become Olig2$^+$ motor neuron progenitors through shh and retinoic acid (RA) signals (Novitch et al., 2003; Diez del Corral et al., 2003). Postmitotic motor neuron generation from Olig2$^+$ progenitors is governed by RA through the induction of GDE2, a six-transmembrane protein with an extracellular glycerophosphodiester phosphodiesterase (GDPD) domain (Novitch et al., 2003; Diez del Corral et al., 2003; Rao and Sockanathan, 2005; Yan et al., 2009; Nogusa et al., 2004). GDE2 is expressed in all somatic motor neurons and synchronizes neurogenic and motor neuron fate specification pathways to drive motor neuron generation through extracellular GDPD activity (Rao and Sockanathan, 2005; Yan et al., 2009). Newly generated motor neurons share generic motor neuron properties that are distinct from neighboring interneurons, such as their use of acetylcholine as a neurotransmitter and the ability of their axons to exit the ventral root. Postmitotic motor neurons subsequently diversify into different motor columns and pools that have distinct positional, molecular, and axonal projection profiles that are fundamental to motor circuit formation (Dasen and Jessell, 2009). The major motor columns in the spinal cord consist of the median motor column (MMC), which spans the entire body axis and innervates dorsal axial muscles; the preganglionic columns (PGCs) and hypaxial motor columns (HMCs), located primarily at thoracic levels, which respectively target the viscera and body wall muscles (Prasad and Hollyday, 1991); and the limb-specific lateral motor columns (LMCs), which are divided into lateral and medial subdivisions that innervate dorsal and ventral limb musculature (Landmesser, 1978; Landmesser, 2001). Medial and lateral LMC motor neurons are further clustered into motor pools according to their projections to individual target muscles (Gutman et al., 1993; Landmesser 1978; Lin et al., 1998).

Current models propose that columnar and pool identities are instructed in newly born motor neurons via intrinsic hierarchical

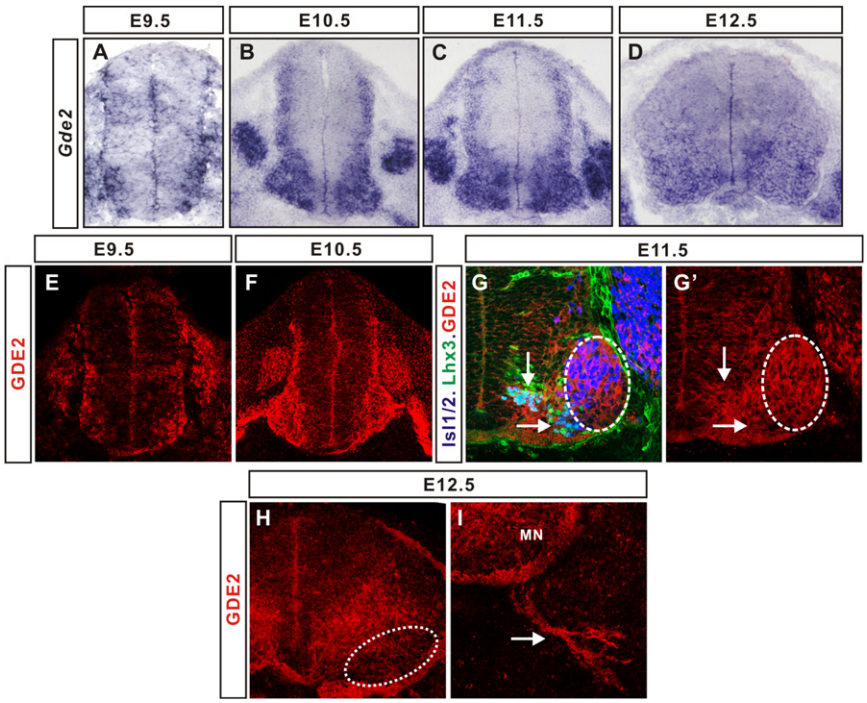

Figure 1. GDE2 Expression in Developing Motor Neurons

(A–D) In situ expression analyses of *Gde2* mRNA on sections of embryonic mouse forelimb spinal cords. *Gde2* transcripts are detected in developing motor neuron cell bodies, dorsal root ganglia, and dorsal-lateral regions of the spinal cord.

(E–I) Confocal images of GDE2 protein expression in mouse spinal cord forelimb sections.

(G and G') GDE2 protein expression in relation to motor neuron columnar markers. GDE2 expression alone is shown in (G') for comparison. Vertical arrow represents newly differentiating motor neurons; horizontal arrow represents MMC; hatched areas represent LMC.

(H and I) Hatched circle marks location of motor neurons (MNs) in the ventral horn at E12.5, which shows weak GDE2 expression; at this stage, GDE2 is enriched in motor axons (arrow).

See also Figure S1.

transcription programs and extrinsic signals. The distinction between MMC and non-MMC motor columns is imposed via ventrally derived Wnt signals (Agalliu et al., 2009), while non-MMC motor columnar identity is directed by early mesodermal sources of graded FGF, retinoid, and TGF$\tilde{\beta}$ -like signals. These pathways ultimately regulate the motor-neuron-specific expression of Hox transcription factors in restricted rostral-caudal domains, where they regulate the expression of transcription factors such as the LIM homeodomain proteins to specify the settling position and axonal projection patterns of prospective LMC and PGC neurons (Dasen and Jessell, 2009; Ji et al., 2009; Shah et al., 2004; Wu et al., 2008; Jung et al., 2010). Hox proteins play principal roles in the formation of motor pools spanning the LMC and within a single spinal segment (Dasen et al., 2005); however, they are not the sole regulators of motor pool identity. Target-derived signals induce the expression of ETS transcription factors such as ER81 and Pea3 within a select subset of motor pools, which subsequently dictate and refine sensorimotor connectivity (Lin et al., 1998; Arber et al., 2000; Haase et al., 2002; Vrieseling and Arber, 2006). Interestingly, alpha and gamma motor neurons appear identical in terms of their gene expression, morphology, and peripheral projections during embryogenesis (Burke et al., 1977; Friese et al., 2009; Kanning et al., 2010). These observations suggest that they initially undergo comparable programs of column- and pool-specific differentiation but diverge prenatally to acquire their individual properties (Friese et al., 2009; Shneider et al., 2009).

The evidence thus far suggests that, in contrast to the mechanisms that instruct the differentiation of different neuronal subclasses within the spinal cord, subtype diversification among motor neurons appears to operate postmitotically (Dasen and Jessell, 2009). However, the ability of certain Hox proteins to influence motor columnar identity through their function in progenitors, as well as observations from neural tube rotation experiments that suggest that motor pool fates are specified at the time of motor neuron progenitor differentiation, raises the possibility that motor neuron subtype diversity is initiated within motor neuron progenitors (Dasen et al., 2003; Matise and Lance-Jones, 1996). In support of this model, we provide here genetic evidence suggesting that newly born motor neurons are not uniform, as previously believed, but are biased from the outset toward particular fates. We show that GDE2 does not regulate the generation of all motor neurons but is required for the timing and generation of distinct LMC motor pools, particularly their alpha motor neuron components. Mechanistically, we show that GDE2 regulates motor neuron differentiation by antagonizing Notch signaling in neighboring motor neuron progenitors through extracellular GDPD activity. These observations define GDE2 as a key regulator of motor neuron diversity through its function in regulating motor neuron progenitor differentiation and suggest that fundamental distinctions between different motor neuron subtypes are imposed earlier than previously appreciated, namely within motor neuron progenitors prior to their differentiation into postmitotic motor neurons.

RESULTS

GDE2 Expression in Spinal Motor Neurons

GDE2 is expressed in motor neurons at all axial levels (Rao and Sockanathan, 2005). To define the developmental profile of *Gde2* expression, we examined the distribution of *Gde2* transcripts in embryonic forelimb spinal cords from E9.5, when motor neurons are first generated, to E12.5, when motor columns have been established. *Gde2* mRNA is detected in somatic motor neurons until E11.5 but is substantially decreased by E12.5 (Figures 1A–1D; data not shown). Consistent with previous studies showing a requirement for GDE2 in interneuron

generation, *Gde2* transcripts extend dorsally from E10.5, coincident with the timing of ventral and dorsal interneuron formation (Figures 1B and 1C; Yan et al., 2009). Similarly, GDE2 protein is expressed in postmitotic somatic motor neurons from E9.5 and is detected dorsally from E10.5 (Figures 1E and 1F). Examination of GDE2 expression in relation to columnar-specific motor neuron markers at fore- and hindlimb levels of the spinal cord shows that GDE2 is localized to newly differentiating motor neurons and to MMC and lateral and medial LMC motor neurons (Figures 1E–1G'; Tsuchida et al., 1994; data not shown). By E12.5, GDE2 protein is reduced within motor neuron cell bodies but is enriched within motor axons, suggesting that GDE2 may have later roles in postmitotic motor neuron development (Figures 1H and 1I). Thus, GDE2 is expressed in somatic motor neuron cell bodies coincident with the period of motor neuron neurogenesis.

GDE2 Is Required for Motor Neuron Formation

To test the requirement for GDE2 in regulating motor neuron generation, we generated stable mouse lines that lack functional GDE2 (*Gde2*$^{-/-}$) using Cre-lox technology (see Figure S1 available online). We confirmed GDE2 ablation using a combination of PCR, direct sequencing, western blot, and immunohistochemical analyses (Figure 7C; Figure S1). Examination of *Gde2*$^{-/-}$ and wild-type (WT) littermates at the onset of motor neuron differentiation at E9.5 showed an approximately 50% loss of Isl1/2^{+} and HB9^{+} motor neurons (Figures 2A, 2B, 2D, 2E, and 2G; Nornes and Carry, 1978). However, the number of Olig2^{+} motor neuron progenitors and the dorsal-ventral patterning of spinal progenitors were not affected (Figures 2C, 2F, and 2G; Figure S2). No increase in TUNEL staining was detected in *Gde2*$^{-/-}$ animals, suggesting that the loss of GDE2 does not compromise motor neuron survival but instead disrupts motor neuron formation (Figure S2). Consistent with this model, *Gde2* null mutants showed a decrease in the number of progenitors exiting the cell cycle (Figures 2J, 2M, and 2N). Although no changes in the proportion of cells in S phase and M phase were detected, the total number of cells in S phase after a 16 hr BrdU pulse was increased, suggesting that the length of the cell cycle is extended in the absence of GDE2 (Figures 2H–2N; Yan et al., 2009). These data collectively support previous findings in the chick showing that GDE2 is required to regulate motor neuron generation but does not affect progenitor patterning and specification (Rao and Sockanathan, 2005).

GDE2 Function Is Restricted to Specific Motor Columns

Some motor neurons are generated in the absence of GDE2, suggesting that GDE2 function might be redundant with its family members *Gde3* and *Gde6* (Nogusa et al., 2004; Yanaka et al., 2003). However, *Gde3* and *Gde6* transcripts do not overlap with *Gde2* mRNA in spinal motor neurons (data not shown). To determine whether GDE2 is required for the generation of motor neurons of distinct subtypes, we examined motor column formation in WT and *Gde2* null littermates (Figure S3; Tsuchida et al., 1994; Rousso et al., 2008; Dasen et al., 2008). At fore- and hindlimb levels, *Gde2* null animals showed an approximately 40%–50% loss of medial and lateral LMC neurons at E11.5 and a decrease of 30%–35% at E13.5 (Figures 3A–3G and 3O–3U), whereas we noted a modest decrease of 20% in thoracic HMC neurons at E11.5 (Figures 3H–3N). Strikingly, no changes in the numbers of MMC neurons or PGC neurons were found at either time point (Figures 3A–3U). The loss of HMC and LMC neurons in *Gde2*$^{-/-}$ animals is unlikely to be due to impaired Hox activities because of the following: (1) gain or loss of Hox gene function does not reduce motor neuron numbers; (2) expression of FoxP1, a critical cofactor of Hox function, in existing motor neurons is unaffected by the loss of GDE2 (Figures 3A–3T; Rousso et al., 2008; Dasen et al., 2008); and (3) brachial Hoxc6, thoracic Hoxc9, and lumbar Hoxa10 expression are preserved in motor neurons of *Gde2*$^{-/-}$ animals (Figure S3; Jung et al., 2010). V2 interneurons derive from Lhx3^{+} progenitors, and V2 interneuron differentiation programs are actively suppressed in motor neurons by the transcription factor HB9 (Arber et al., 1999; Thaler et al., 1999; Thaler et al., 2002). Islet1/2 motor neurons did not coexpress Chx10, no increases in cell death by TUNEL were detected, and V2 interneuron numbers were unchanged in the absence of GDE2, arguing against the possible conversion of prospective HMC and LMC neurons to V2 fates (Figures S2 and S3; data not shown).

Taken together, these observations suggest that GDE2 function is restricted to the formation of LMC and HMC motor neurons and invokes the existence of other regulatory modules that control the formation of GDE2-independent motor neurons.

GDE2 Is Required for the Differentiation of Specific Motor Pools

The loss of fore- and hindlimb LMC neurons in *Gde2*$^{-/-}$ animals indicates that GDE2 activity is not restricted to a specific rostral-caudal domain, whereas the partial reduction of medial and lateral LMC neurons suggests that GDE2 might be required for the formation of distinct LMC motor pools (Figure 3). We analyzed *Gde2* null animals at lumbosacral segment (LS) 2 of the spinal cord, where combined molecular and axonal tracing approaches have defined a molecular code that distinguishes seven medial and lateral LMC motor pools that innervate major muscle groups in the hindlimb (Figure 4C; De Marco Garcia and Jessell, 2008; Lin et al., 1998; Arber et al., 2000). These include five motor pools within the medial LMC that innervate the adductor longus and magnus (Al, Am), the adductor brevis (Ab), and the anterior and posterior gracilis muscles (Ga, Gp), as well as two lateral LMC pools that target the vasti (Va) and the rectofemoratibialis muscles (Rf). We assigned motor neurons to specific motor pools based on their position along the dorsal-ventral and medial-lateral axes and their unique molecular identity in terms of two separate molecular codes (Figure 4C).

Analysis of the LS2 LMC motor pools in *Gde2*$^{-/-}$ animals at E13.5 and E14.5 showed a dramatic reduction of the medial Ga motor pool (dorsal green cells in Figures 4A and 4B) and a 60%–70% reduction of medial Ab motor neurons (Figures 4A–4C, 4E–4J, and 4L). Furthermore, we detected a 60%–70% reduction in the lateral Va motor pool at E13.5 and E14.5 (Figures 4A–4C and 4I–4K) and a 40%–50% reduction in the Rf motor pool at E13.5 (Figures 4C, 4D, 4M, and 4N). The bona fide loss of these motor pools in *Gde2*$^{-/-}$ animals is further substantiated

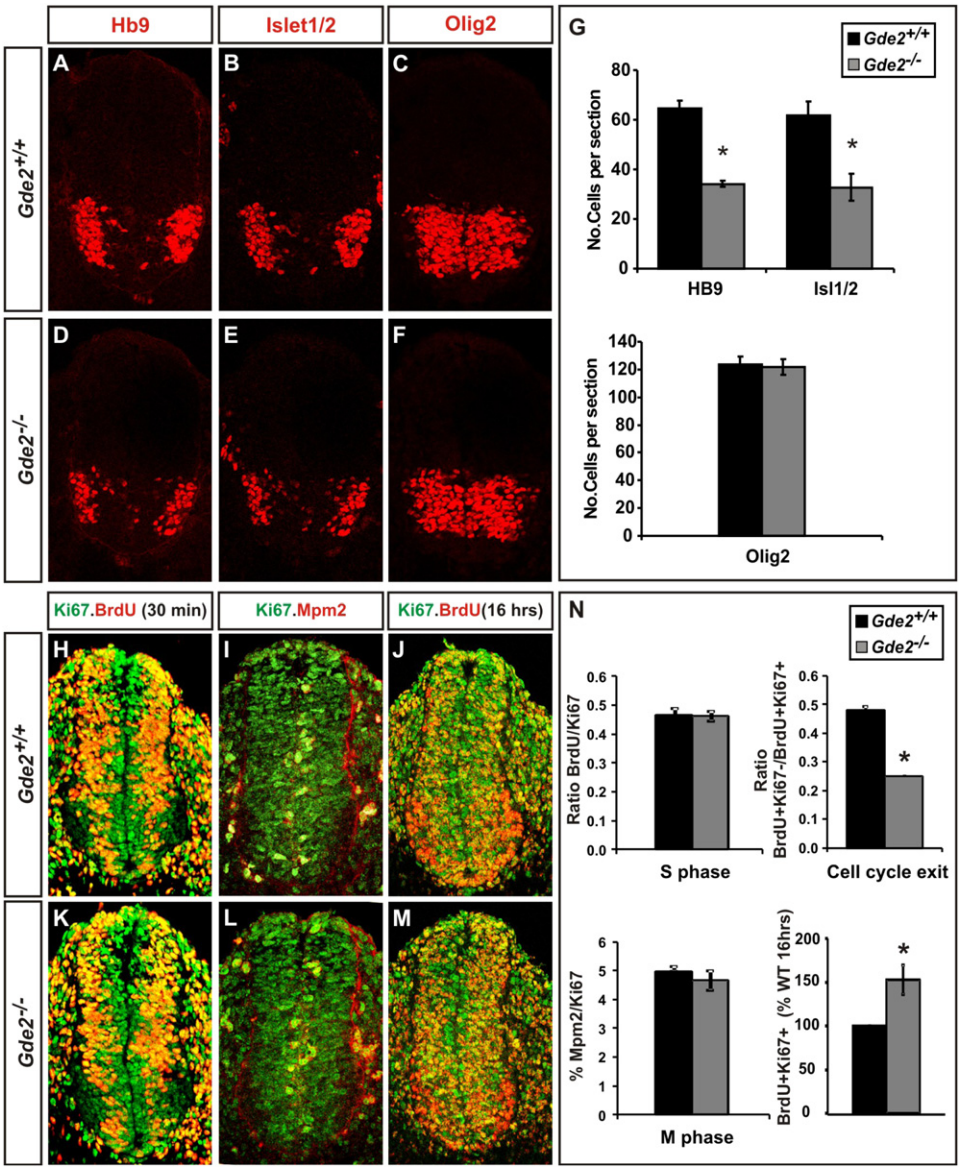

Figure 2. GDE2 Is Required for Motor Neuron Generation

(A–F and H–M) Confocal images of sections of E9.5 mouse spinal cord.

(H, J, K, and M) S phase and cell-cycle-exit indices were calculated 30 min and 16 hr after BrdU injections, respectively.

(G) Graphs quantifying HB9$^+$ and Isl1/2$^+$ motor neurons and Olig2$^+$ motor neuron progenitors (HB9 *p = 0.0014; Isl1/2 *p = 0.004; Olig2 p = 0.3; n = 5).

(N) Graphs of S phase, M phase, cell-cycle-exit indices, and total number of S phase cells after 16 hr BrdU pulse (S phase p = 0.91; cell-cycle exit *p = 0.0005; M phase p = 0.37; total S phase (18 hr) *p = 0.03; n = 4).

All graphs represent mean ± standard error of the mean (SEM), Student's t test. See also Figure S2.

by the absence of Isl2$^+$/Lhx1$^+$ and Foxp1$^+$/Isl2$^+$ lateral LMC motor neurons in adjacent sections; the observation that medial Ab and lateral Va motor neurons could not be detected in *Gde2*$^{-/-}$ animals from the time of Ab and Va motor pool formation at E12.5 and from EdU birth-dating studies shows that many Ab and Va motor neurons are not born in the absence of GDE2 (Figure S4; data not shown). Further, TUNEL labeling was equivalent between WT and *Gde2*$^{-/-}$ animals from E9.5 to E14.5, arguing for deficits in motor neuron generation rather than survival in the absence of GDE2 (Figure S2).

In contrast, the numbers of neighboring Al, Am, and Gp medial LMC motor neurons were decreased at E12.5 in *Gde2*$^{-/-}$ embryos but were equivalent to controls at E13.5 and E14.5 (Figures 4A–4C, 4G, 4I, and 4J; Figure S4). Visualization of the major axonal tracts emerging from LS2 using *HB9-GFP* transgenic animals showed that they appeared thinner in *Gde2*$^{-/-}$ animals, consistent with a loss in motor neuron numbers (Figure S4; Huber et al., 2005). However, existing LMC neurons showed no obvious deficits in motor axon extension at E12.5 and E14.5 and were capable of forming

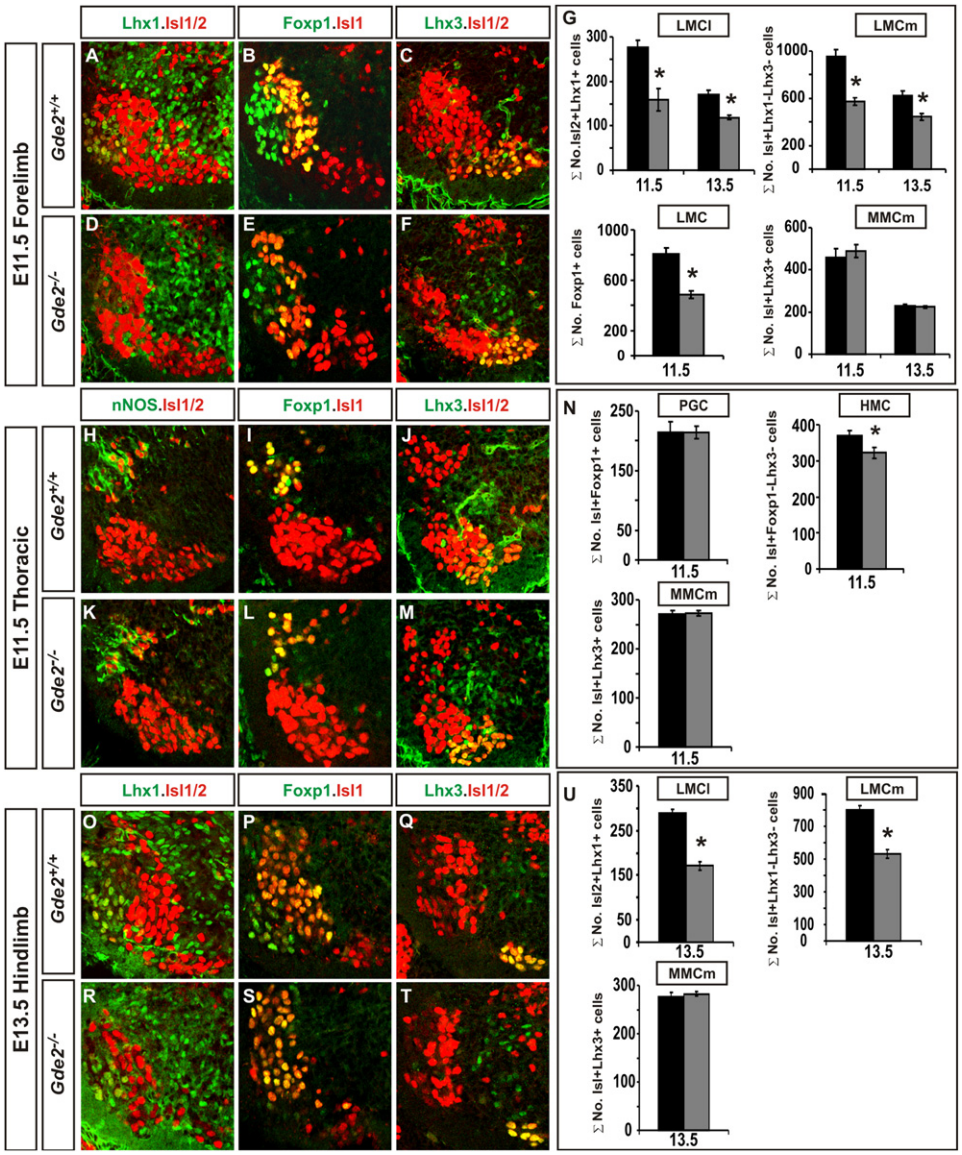

Figure 3. GDE2 Function Is Columnar Specific

(A–F, H–M, and O–T) Confocal images of ventral left quadrant of sections of E13.5 mouse spinal cords.

(G) Graphs quantifying total motor neurons in E11.5 and E13.5 forelimb motor columns (LMCl E11.5 *p = 0.001, E13.5 *p = 0.005; LMCm E11.5 *p = 0.002, E13.5 *p = 0.004; LMC E11.5 *p = 0.001; MMC E11.5 p = 0.205, E13.5 p = 0.374).

(N) Graphs quantifying total motor neurons in E11.5 thoracic motor columns (PGC p = 0.94; HMC *p = 0.01; MMC p = 0.64).

(U) Graphs quantifying total motor neurons in E13.5 hindlimb motor columns (LMCl *p = 0.0004; LMCm *p = 0.0006; MMC p = 0.664).

All graphs represent mean ± SEM, Student's t test, n = 4. See also Figure S3.

neuromuscular junctions (Figure S4; data not shown). These observations argue against the possibility that target-derived Pea3 and Er81 expression that marks these pools was delayed due to stunted axonal outgrowth or failure in synaptogenesis (Figure S4; data not shown). Instead, consistent with a delay in their formation, birth-dating studies using timed injection of EdU showed that the Al, Am, and Gp pools were born later in *Gde2*$^{-/-}$ animals compared with WT littermates (Figure S4).

Taken together, our results suggest that GDE2 regulates the timing of formation of medially located Al, Am, and Gp motor pools and is necessary for the generation of prospective Ab, Ga, Va, and Rf motor neurons. Our data argue against the likelihood that the loss of motor pools is due to disrupted Hox function, because the Al, Am, and Gp motor pools were not expanded as a consequence of Ab, Ga, Va, and Rf reduction in *Gde2*$^{-/-}$ animals. Moreover, the expression of the Hox downstream target gene, Nkx6.1, in existing motor neurons is unaffected by GDE2 elimination (Figures 4E–4G, 4I, and 4J; De Marco Garcia and Jessell, 2008; Dasen et al., 2003).Because motor pools emerge in the context of individual columns, our

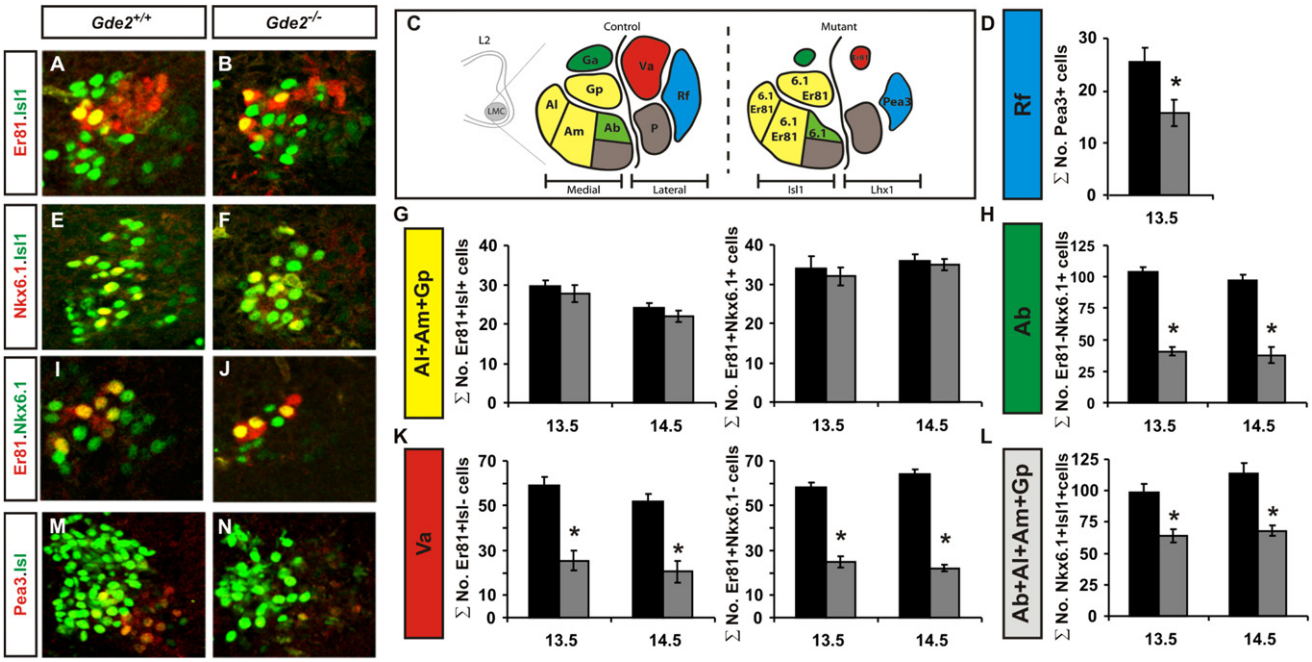

Figure 4. GDE2 Function Is Restricted to Specific LMC Motor Pools

(A, B, E, F, I, J, M, and N) Confocal images of ventral left quadrant of E14.5 mouse LS2 spinal cord sections.

(C) Schematic of distribution and molecular code of LS2 motor pools.

(D, G, H, K, and L) Graphs quantifying total motor neurons within E13.5 and E14.5 motor pools (Pea3 *p = 0.0014; Al + Am + Gp [Er81$^+$ Isl1$^+$] E13.5 p = 0.449, E14.5 p = 0.356, [Er81$^+$ Nkx6.1$^+$] E13.5 p = 0.67, E14.5 p = 0.815; Ab [Er81$^-$Nkx6.1$^+$] E13.5 *p = 0.013, E14.5 *p = 0.007; Va [Er81$^+$ Isl1$^-$] E13.5 *p = 0.0001, E14.5 *p = 0.005, [Er81$^+$ Nkx6.1$^-$] E13.5 *p = 0.004, E14.5 *p = 0.002; Ab + Al + Am + Gp E13.5 *p = 0.004, E14.5 *p = 0.006).

All graphs represent mean ± SEM, Student's t test, E13.5 n = 4, E14.5 n = 5. See also Figure S4.

data suggest that GDE2 controls the formation of motor neurons with specific columnar and pool identities.

GDE2 Ablation Compromises Alpha Motor Neuron Differentiation

We noted that 30%–40% of motor neurons are preserved in laterally located LMC motor pools in the absence of GDE2 at E13.5. This number is remarkably similar to that reported for the gamma motor neuron component of motor pools, which are predicted to begin diversifying from alpha motor neurons by E13.5, given their differential sensitivities to embryonic programmed cell death (Burke et al., 1977; Friese et al., 2009; Buss et al., 2006; Hui et al., 2008). To examine whether GDE2 selectively regulates the differentiation of alpha, but not gamma, motor neurons, we compared *Gde2*$^{-/-}$ animals with WT siblings at postnatal day 5 (P5) and P28, when molecular and somal size differences allow alpha and gamma motor neurons to be distinguished (Friese et al., 2009). The percentage of ChAT$^+$/NeuN$^+$ alpha motor neurons in the ventral outer quadrant of the spinal cord corresponding to the LMC was decreased by approximately 30%–40% at P5 and P28 in *Gde2*$^{-/-}$ animals; however, the percentage of ChAT$^+$/NeuN$^-$ gamma motor neurons was not significantly altered (Figures 5A–5F). The expression of *Err3* in the ventral horn of the spinal cord appeared to be similar between *Gde2*$^{-/-}$ and WT littermates, consistent with preserved gamma motor neuron differentiation in the absence of GDE2 (Figures 5G and 5H). Gamma motor neurons have a small somal area compared with alpha motor neurons (Burke et al., 1977; Friese et al., 2009; Shneider et al., 2009). The number of putative gamma motor neurons (somal area < 380 μm^2) was unchanged between WT and *Gde2*$^{-/-}$ littermates, but there was a dramatic reduction of putative alpha motor neurons in *Gde2*$^{-/-}$ animals (somal area = 380–1,400 μm^2) (Figures 5I and 5J). Using the same criteria discussed above, no significant changes in alpha and gamma motor neuron numbers were observed in the medially located MMC of *Gde2*$^{-/-}$ and WT animals (Figures 5K–5O).

Thus, the reduction in LMC motor pools in *Gde2* null animals correlates with a specific loss of alpha motor neurons, whereas LMC gamma motor neurons and MMC alpha and gamma motor neuron production are intact.

Ablation of GDE2 after Neurogenesis Does Not Impair Motor Pool Formation

At hindlimb levels, GDE2 is first localized to motor neuron cell body areas at the time of motor neuron generation but is subsequently enriched in motor axons from E12.5 (Figure 6B; Figure S5). To define when GDE2 functions in hindlimb motor pool formation, we generated *Gde2*$^{lox/-}$; *Rosa26:CreER*$^+$ animals, which enabled the timed ablation of GDE2 through Cre-dependent recombination via the administration of 4-hydroxytamoxifen (4-OHT) (Badea et al., 2003). We injected pregnant dams with 4-OHT at E8.5 to ablate GDE2 expression prior to the initiation of motor neuron progenitor differentiation at lumbar levels

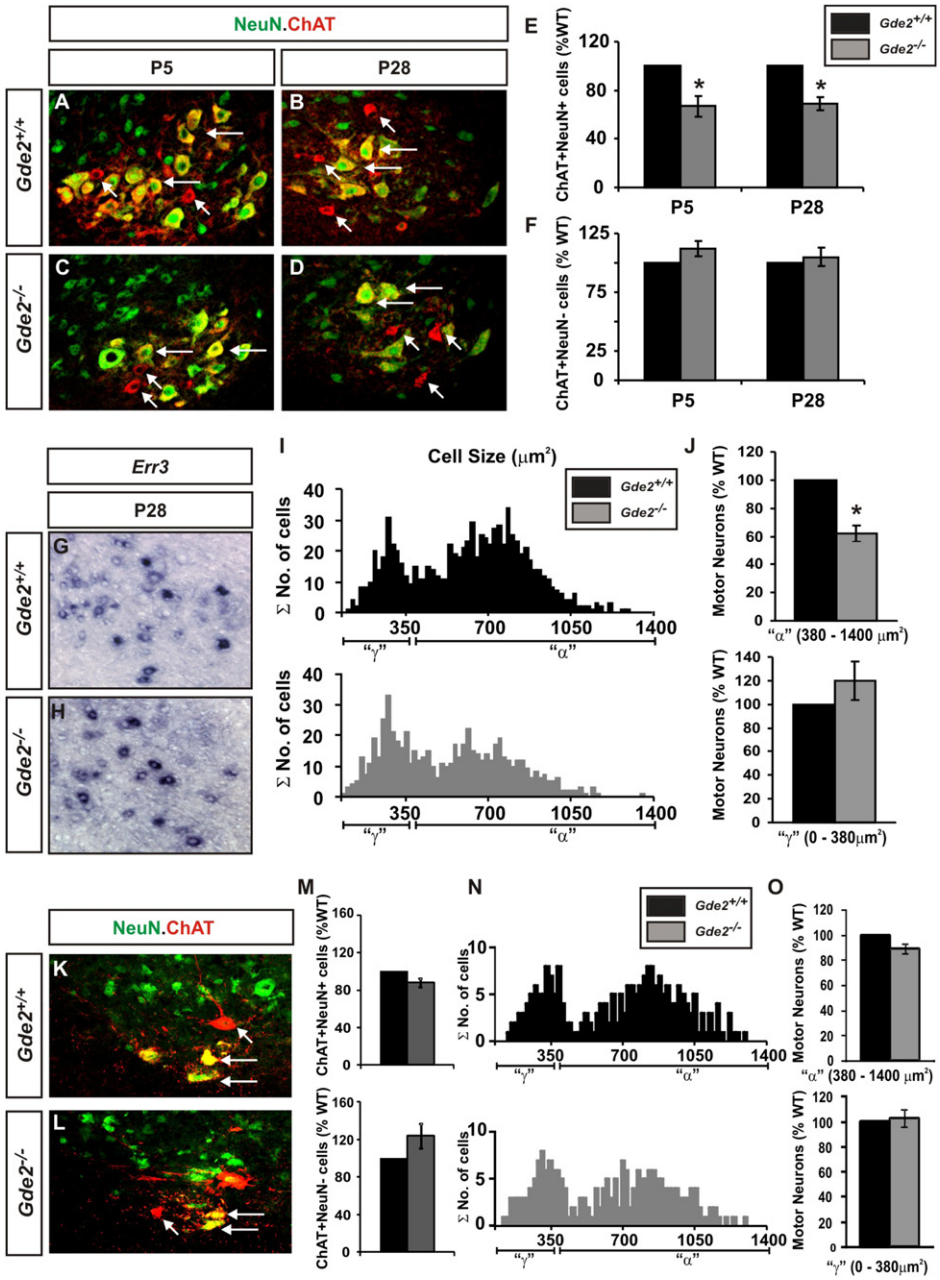

Figure 5. GDE2 Is Required for LMC Alpha Motor Neuron Differentiation

(A–D, K, and L) Confocal images of ventral right quadrants of sectioned mouse spinal cords showing lateral (A–D) and medial (K and L) motor neurons. Horizontal arrows represent alpha (α) motor neurons. Angled arrows represent gamma (γ) motor neurons.

(E and F) Graphs quantifying percentage lateral (P5 *p = 0.009, P28 *p = 0.007 [E]; P5 p = 0.56, P28 p = 0.45 [F]) and medial motor (M, $Chat^{+}NeuN^{+}$ p = 0.09, $Chat^{+}NeuN^{-}$ p = 0.19) neurons.

(G and H) In situ hybridization analyses of sectioned lateral ventral horns of spinal cord.

(I) Histograms of somal cell area of $ChAT^{+}$ lateral motor neurons at P28 (n = 845 cells). Average somal areas (mean [μ]): $Gde2^{+/+}$: putative α motor neurons = 703.04 ± 196.64 μm^2 [SD (σ)], putative γ motor neurons = 239.47 ± 69.7 μm^2; $Gde2^{-/-}$: putative α motor neurons = 609.04 ± 210.17 μm^2, putative γ motor neurons = 246.34 ± 96.4 μm^2.

(J and O) Graphs quantifying percentage putative γ and α motor neurons according to somal area. Threshold cutoff sizes for lateral and medial γ motor neuron populations were estimated at 380 μm^2 in cell area (μ + 2σ of the fitted small population distribution in controls). α motor neurons *p = 0.0004, γ motor neurons p = 0.3 (J); α motor neurons p = 0.69; γ motor neurons p = 0.1 (O).

(N) Histograms of somal cell area of $ChAT^{+}$ medial motor neurons at P28 (n = 229 cells). Average somal areas: $Gde2^{+/+}$: putative α motor neurons = 818.33 ± 196 μm^2, putative γ motor neurons = 268.05 ± 84.56 μm^2; $Gde2^{-/-}$: putative α motor neurons = 794.51 ± 207.93 μm^2, putative γ motor neurons = 267.36 ± 86.68 μm^2.

All graphs represent mean ± SEM, One sample t test, n = 4.

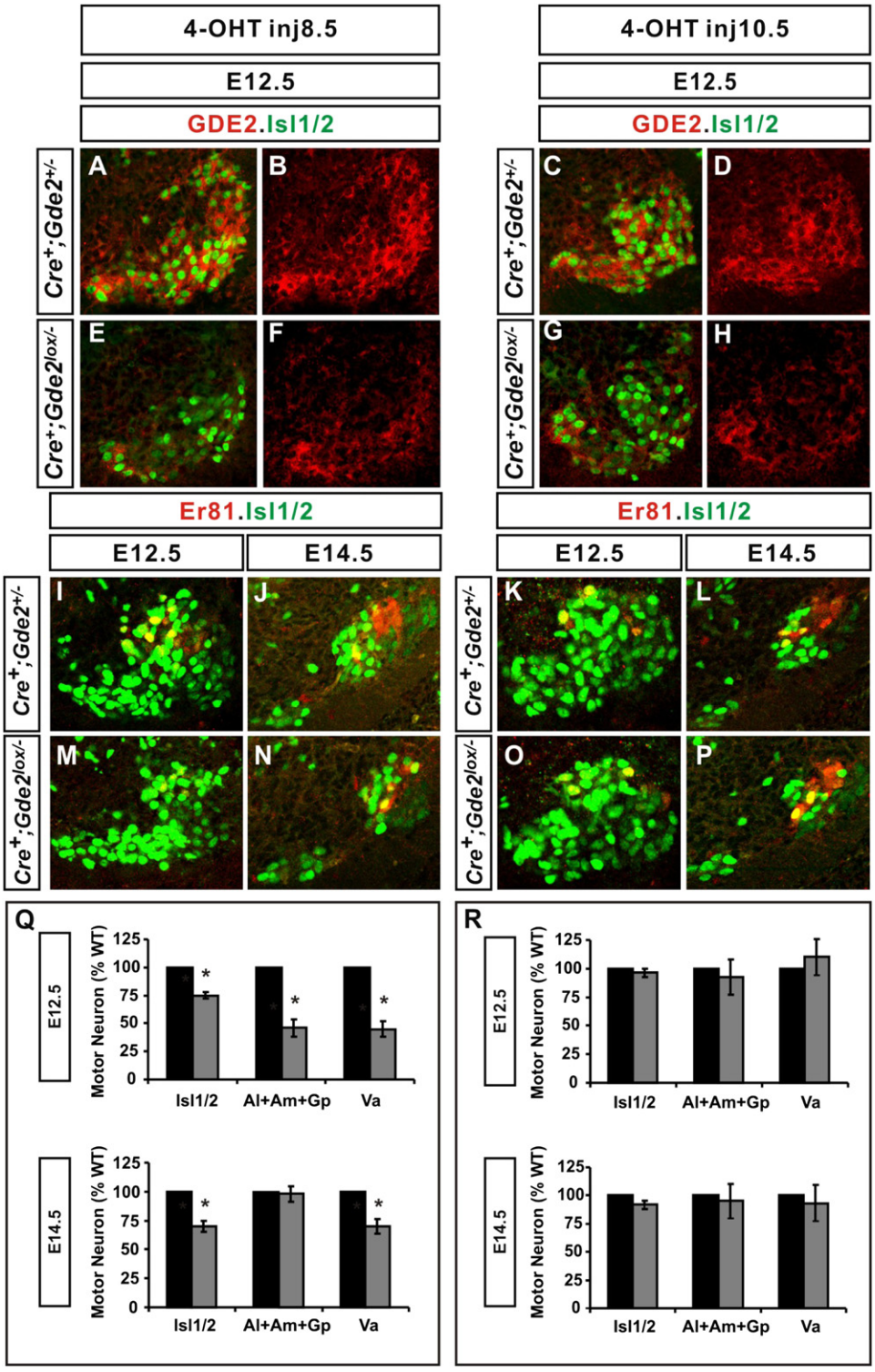

Figure 6. GDE2 Functions during the Period of Motor Neuron Generation

(A–P) Confocal images of ventral right quadrant of mouse LS2 spinal cord sections at E12.5, except where stated.

(Q and R) Graphs quantifying the percentage of motor neurons within E12.5 and E14.5 motor pools. Black bar: *Cre*$^{+}$*; Gde2*$^{+/-}$; gray bar: *Cre*$^{+}$*; Gde2*$^{lox/-}$ (E12.5 Isl1/2 *p = 0.0002, Al + Am + Gp *p = 0.007, Va *p = 0.001; E14.5 Isl1/2 *p = 0.0017, Al + Am + Gp p = 0.75, Va *p = 0.02 [Q]. E12.5 Isl1/2 p = 0.382, Al + Am + Gp p = 0.509, Va p = 0.761; E14.5 Isl1/2 p = 0.255, Al + Am + Gp p = 0.477, Va p = 0.676 [R]).

All graphs represent mean ± SEM, one sample t test, n = 3. See also Figure S5.

and at E10.5 to eliminate GDE2 by the end of motor neuron generation (Nornes and Carry, 1978).

Gde2$^{lox/-}$; *Rosa26:CreER*$^{+}$ embryos from pregnant dams injected with 4-OHT at E8.5 or E10.5 showed an equivalent loss of GDE2 in motor neuron cell bodies and axons at E12.5, demonstrating that Cre-mediated loss of GDE2 in both cases had occurred prior to detectable LS2 motor pool formation (Figures 6B, 6D, 6F, and 6H; Figure S5). Analysis of the Va, Al, Am, and Gp motor pools in *Gde2*$^{lox/-}$; *Rosa26:CreER*$^{+}$ embryos after 4-OHT injection at E8.5 showed a loss of Isl1/2^{+} motor neurons and a dramatic reduction of ER81^{+} Va motor neurons at E12.5 and E14.5 compared with *Gde2*$^{lox/-}$ and *Gde2*$^{+/-}$; *Rosa26:CreER*$^{+}$ controls (Figures 6I–6Q; data not shown). Consistent with the phenotype of *Gde2* null animals, Al, Am, and Gp pool formation was delayed such that a decrease in Er81/Isl1^{+} motor neuron numbers at E12.5 was mitigated by E14.5 (Figures 6I–6Q). Thus, elimination of GDE2 prior to the initiation of motor neuron generation mimics the phenotype observed in *Gde2* null animals. In contrast, administration of 4-OHT at E10.5 did not alter the number of Va, Al, Am, or Gp motor neurons in *Gde2*$^{lox/-}$; *Rosa26:CreER*$^{+}$ embryos compared with *Gde2*$^{lox/-}$ and *Gde2*$^{+/-}$; *Rosa26:CreER*$^{+}$ controls, although the level of GDE2 ablation was equivalent in both cases (Figures 6F, 6H, 6K, 6L, 6O, 6P, and 6R; Figure S5).

These results suggest that GDE2 removal at the onset of neurogenesis disrupts the formation of specific motor pools, whereas GDE2 ablation after motor neuron generation is complete does not. Thus, the ability of GDE2 to regulate the formation of specific LMC motor pools coincides precisely with the temporal profile of motor neuron neurogenesis and the localization of GDE2 within motor neuron cell bodies and dendrites.

GDE2 Is Necessary and Sufficient to Inhibit Notch Signaling

To determine how GDE2 regulates motor neuron differentiation, we considered the possibility that GDE2 might downregulate Notch signaling, a pathway known to be required for the maintenance of Olig2^{+} motor neuron progenitors in an undifferentiated state (Marklund et al., 2010). To test this hypothesis, we compared the expression of two direct downstream targets of activated Notch in *Gde2*$^{-/-}$ spinal cords in relation to WT littermates. *Gde2*$^{-/-}$ animals showed a marked expansion of *Hes5* and *Blbp* expression (Figures 7A, 7B, 7D, and 7E); further, GDE2 ablation increased the amount of Notch intracellular domain (NICD) in dissected ventral spinal cords, in accordance with elevated levels of ligand-dependent Notch processing and an increase of activated Notch signaling (Figure 7C; Peng et al., 2007). These data collectively suggest that GDE2 is necessary to downregulate Notch signaling in neighboring motor neuron progenitors. To determine whether GDE2 is sufficient to inhibit Notch signaling, we utilized a gain-of-function approach using in ovo electroporation of embryonic chick spinal cords. Confirming and extending previous studies, overexpression of GDE2 caused Olig2^{+} progenitors in the VZ to precociously differentiate into Isl2^{+} motor neurons, whereas versions of GDE2 mutated within the GDE2 GDPD domain (GDE2.APML) failed to do so (Figure 7F; Rao and Sockanathan, 2005). Embryos electroporated with GDE2 showed a concomitant reduction of *Hes5* and *Blbp* expression, whereas GDE2.APML electroporation did not (Figures 7J–7O). These observations suggest that GDE2 is sufficient to inhibit Notch activity and induce motor neuron differentiation and that this function is dependent on its extracellular GDPD activity. Consistent with this observation, electroporation of a dominant-negative (dn) version of the NICD transcriptional coactivator MAML effectively induced Isl2^{+} motor neuron differentiation in the VZ, synonymous with GDE2 overexpression (Figures 7F–7G'; Peng et al., 2007), and coexpression of NICD and GDE2 was sufficient to inhibit GDE2-dependent induction of motor neuron differentiation in VZ progenitors (Figures 7H and 7I).

GDE2 is expressed in newly differentiating motor neurons in the IZ, predicting that GDE2 functions non-cell-autonomously to inhibit Notch signaling in neighboring Olig2^{+} progenitors. Previous studies have attributed cell- and non-cell-autonomous functions for GDE2 in motor neuron differentiation, but definitive assessment of GDE2 function is lacking due to insufficient cellular resolution of GDE2-dependent motor neuron differentiation (Rao and Sockanathan, 2005; Yan et al., 2009). To better define the autonomy of GDE2 function at single-cell resolution, we utilized established Cre-lox approaches to drive high levels of GDE2 and LacZ expression into a sparse number of VZ progenitors in the chick spinal cord from bicistronic constructs (Zhuang et al., 2009). We observed a 1:1 correlation with LacZ and GDE2 expression, indicating that LacZ is an accurate readout of cells expressing exogenous GDE2 (data not shown). Under these conditions, over 80% of induced Isl2^{+} neurons in the VZ did not express LacZ but instead were located directly adjacent to LacZ^{+} cells, suggesting that cell-cell contact is necessary for non-cell-autonomous induction of motor neuron differentiation by GDE2 (Figures 7P–7R). Further, Isl2^{+} cells that coexpressed LacZ were only detected when in contact with LacZ^{+} cells and were never in isolation (Figures 7Q and 7R). Taken together, these observations are consistent with a non-cell-autonomous function for GDE2 in triggering motor neuron differentiation.

DISCUSSION

Current models suggest that newly born motor neurons are initially a blank slate in terms of subtype identity and that motor columnar and pool fates are instructed in these generic newborn motor neurons by Hox transcriptional programs and extrinsically derived signals (Dasen and Jessell, 2009). Our analyses of GDE2 function prompt these concepts to be reexamined. We show here that GDE2 does not regulate the production of all motor neurons but that GDE2 is required for the timing and formation of motor neurons of defined columnar and pool-specific identities. Strikingly, postmitotic Hox protein expression and activities are not directly affected by GDE2. Instead, GDE2 downregulates Notch signaling pathways in neighboring progenitor cells through a non-cell-autonomous mechanism that depends on extracellular GDE2 GDPD activity. This mechanism of GDE2 function is consistent with our observations that ablation of GDE2 decreases progenitor cell-cycle exit, prolongs the mitotic cell cycle, delays the birth of prospective medially located LMC motor pools, and results in the failure of lateral motor pool

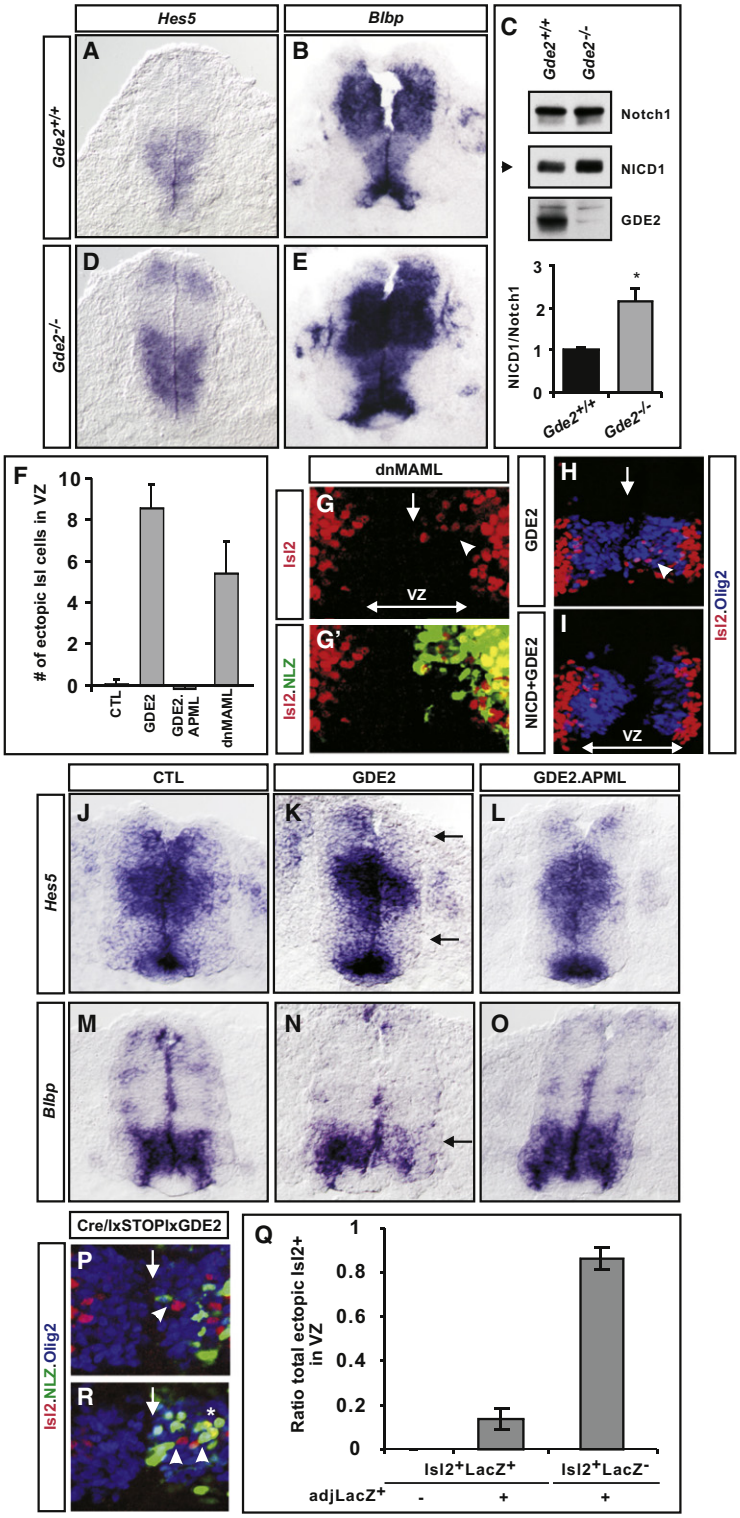

Figure 7. GDE2 Inhibits Notch Signaling

(A, B, D, and E) In situ hybridizations of transverse sections of E9.5 (A and D) and E10.5 (B and E) mouse and electroporated chick spinal cords at HH St 19.

(C) Western blot of dissected E10.5 spinal cord extracts from *Gde2*$^{-/-}$ embryos and WT littermates. Graph shows densitometric quantitation of NICD/full-length Notch ratios from western blots; *p = 0.035, n = 4.

(F) Graph shows average number of ectopic Isl2^{+} motor neurons/section in VZ of electroporated chick spinal cords; n = 8–10.

(G, G', H, and I) Confocal images of transverse sections of chick spinal cords electroporated on the right. VZ, ventricular zone; vertical arrow, midline. Arrowheads mark ectopic Isl2^{+} motor neurons.

(J–O) Expression of *Hes5* and *Blbp* transcripts. Arrows mark areas of Notch inhibition.

(P and R) Two examples of chick spinal cords electroporated on the right with Lox-STP-Lox GDE2 and CMV:Cre plasmids. Green cells express GDE2; neighboring red cells are progenitors that have differentiated into Isl2^{+} motor neurons. Asterisk (*) in (R) marks Isl2^{+} cells expressing GDE2.

(Q) Graph quantifying ectopic Isl2^{+} motor neurons with respect to LacZ GDE2^{+} cells; n = 161 cells.

All graphs represent mean ± SEM, Student's t test. Statistical analyses using a simple binomial distribution showed that the results we obtained cannot be explained by chance (see Supplemental Experimental Procedures). See also Figure S6.

formation. Thus, GDE2 regulates the generation of specific motor neuron subtypes through its role in triggering the differentiation of motor neuron progenitors into postmitotic motor neurons (Figure S6).

These findings have several implications. First, they suggest that signals from postmitotic motor neurons are required for the formation of specific motor neuron subtypes at the level of motor neuron progenitor differentiation, a previously unrecognized concept in existing models of motor neuron diversification. In our model, MMC motor neurons, which are born prior to LMC neurons and which do not require GDE2 for their formation, serve as an initial source of GDE2 that regulates the progressive generation of prospective LMC motor neurons from adjacent motor neuron progenitors. This function also applies to forelimb regions, because GDE2 is differentially required for the formation of C7-8 Pea3^{-} Scip1^{+} and Pea3^{+} motor pools (P.S. and S.S., unpublished data). This strategy for building complexity within motor neuron populations is particularly compelling because the MMC is thought to be the ancestral motor column, whereas the LMC is a more recent structure that evolved in accordance with limb development (Fetcho, 1992; Dasen et al., 2008). Feedback signaling mechanisms from postmitotic neurons to progenitor cells have been reported to control differentiation in other structures such as the cortex, where signals from cortical neurons can influence astrocyte generation during the neuronal-to-glial switch (Namihira et al., 2009; Seuntjens et al., 2009). Our finding that feedback signals also control subtype identity within a single class of neurons suggests that this strategy may form a general mechanism to control cell diversity in the developing nervous system.

A second implication from this study is that newly born motor neurons are unlikely to be generic as previously believed, given their differential requirements for GDE2 for their generation, but are inherently biased toward distinct postmitotic fates. The ability of Hox proteins to alter motor neuron identities in postmitotic motor neurons implies that such fates are not hard wired but are plastic to some degree. We suggest that hierarchical Hox transcriptional programs and additional signals act to consolidate and refine critical columnar and motor pool properties in newly born motor neurons, thus ensuring appropriate connectivity and function of motor circuits over time (Dasen et al., 2003; Dasen et al., 2005; Jung et al., 2010). Conceptually, this model suggests that elements of postmitotic motor neuron identity are encoded in progenitor cells prior to their differentiation into postmitotic motor neurons and implies that motor neuron progenitors are not uniform but are specified toward distinct postmitotic fates. While our data indicate that such specification includes columnar and pool identities, they also raise the possibility that alpha and gamma motor neuron identities might be encoded within motor neuron progenitors. This hypothesis stems from two observations: first, that the specific loss of LMC alpha motor neurons in postnatal *Gde2*$^{-/-}$ animals correlates with the embryonic phenotype, in which the formation of specific LMC motor pools is compromised while MMC motor neurons are unchanged; and second, that the reduction of LMC alpha motor neurons is highly unlikely to be a consequence of altered sensory neuron and interneuron formation in the absence of GDE2, because previous studies show that these neuronal subtypes are dispensable for alpha motor neuron formation and function (reviewed by Grillner and Jessell, 2009). However, further study is required to test this hypothesis, because our studies do not exclude alternative interpretations that are independent of progenitor specification. For instance, alpha motor neuron differentiation is predicated on the total number of motor neurons within a motor pool, but gamma motor neuron differentiation is not. Nevertheless, our data collectively suggest that, similar to mechanisms that direct the diversification of different neuronal classes within the spinal cord, the acquisition of motor neuron subtype identity is a dynamic and progressive process that is initiated in motor neuron progenitors and continues in postmitotic motor neurons in accordance with their axial position relative to their final targets.

Our analysis of GDE2 function indicates that GDE2 triggers neighboring motor neuron progenitors to undergo differentiation by GDPD inhibition of Notch signaling. Notch signaling maintains the proliferative state of progenitor cells in part by inhibiting the expression of proneural genes such as Mash1 and Ngn2 (reviewed by Corbin et al., 2008). Ngn2 in particular plays pivotal roles in synchronizing neurogenesis and motor neuron specification by decreasing Olig2:Ngn2 ratios to promote neuronal differentiation and by directly interacting with Lhx3 and Isl1 to regulate the transcription of motor neuron-specific genes (Lee and Pfaff, 2003). Overexpression of GDE2 in the chick spinal cord is sufficient to induce ectopic Ngn2 expression, supporting the model that GDE2 promotes motor neuron differentiation via the derepression of Notch-dependent Ngn2 inhibition (M.R. and S.S., unpublished data). It is widely accepted that Notch signaling plays important roles in generating diversity in neural progenitors. For example, differential Notch activity plays central roles in the sequential specification and binary fate choices of progenitors in the *Drosophila* peripheral nervous system, as well as in maintaining the heterogeneity of mammalian cortical progenitors (reviewed in Corbin et al., 2008). Accordingly, it is possible that differential Notch signaling could similarly encode aspects of postmitotic motor neuron subtype identity in motor neuron progenitors and that GDE2-dependent downregulation of Notch signaling could control the differentiation of pool-specific motor neurons. How GDE2 controls the temporal formation of medial LMC neurons via inhibition of Notch signals is less clear. The difference in GDE2 function in terms of regulating the timing of medially located LMC pool formation versus its requirement for the generation of laterally located motor neuron pools correlates with their birth dates, because medial motor pools are born earlier than lateral pools (Nornes and Carry, 1978; Whitelaw and Hollyday, 1983). We speculate that the levels of GDE2 targets might vary over time such that the precise modulation of Notch signaling could directly influence both motor neuron fates and birth dates.

Two major questions that emerge from this work are (1) what are the direct targets of GDE2 GDPD activity? and (2) how do they affect Notch signaling? Definitive identification of GDE2 GDPD substrates is currently underway; however, potential candidates are known from studies in nonneural cells, in which GDE2 metabolizes glycerophosphocholine into glycerol-3-phosphate and choline (Gallazzini et al., 2008). However, it is still unclear whether glycerophosphocholine is indeed the physiological substrate for GDE2 and, if so, how its metabolism could specifically inhibit Notch signaling. Further elucidation of the molecular mechanisms involved will provide key insight into how motor neuron diversity is generated and may define general principles that underlie the regulation of neuronal differentiation in the developing nervous system.

EXPERIMENTAL PROCEDURES

Generation of Gde2 Mutant Mice

Linearized targeting constructs were electroporated into 129/Sv ES cells to generate neomycin-resistant clones (Ingenious Targeting Laboratories), which were screened for potential recombinants by PCR and then confirmed by Southern blot analysis. A 750 bp EcoRI fragment upstream of the targeted region was used as a probe to detect a 4 kb WT band and a 2 kb band for the correctly targeted allele upon BamH1 digestion. Recombinant clones were injected into C57BL/6J blastocysts to produce chimeric founders and were crossed with C57BL/6J animals to obtain germline transmission. Details of primers used for genotyping are described in Supplemental Experimental Procedures. *Gde2*$^{lox/+}$ mice were bred to lines that express Cre recombinase in germline cells to generate *Gde2*$^{+/-}$ mice. *Gde2*$^{+/-}$ animals were intercrossed to generate *Gde2*$^{-/-}$ null mutants, which were born at the expected Mendelian frequency and were viable and fertile. Analyses were carried out on embryos derived from *Gde2*$^{+/-}$ heterozygous intercrosses (mixed 129/Sv × C57BL/6J background).

Motor Neuron Counts

In ovo electroporation of chick embryos was carried out as described (Yan et al., 2009). Cell counts were performed on 10–20 sections from three to five embryos in each instance using ImageJ software. Details are provided in Supplemental Experimental Procedures.

In Situ Hybridization and Immunofluorescence

In situ hybridization and immunostaining experiments were carried out as described (Rao and Sockanathan, 2005). Confocal images were acquired with a Zeiss LSM 5 PASCAL microscope. The m*Gde2* (680 bp) and m*Err3* (776 bp) in situ probes were generated from the 3′UTR region of each gene. Bright-field images were captured on a Zeiss Axioskop2 microscope. Details of antibodies are provided in the Supplemental Experimental Procedures. TUNEL analysis was carried out using the ApopTag fluorescein in situ apoptosis detection kit (Chemicon S7110). Whole-mount GFP staining was performed as described (Huber et al., 2005) and eGFP-labeled motor axons were visualized in projections of confocal Z stacks (500–700 μm).

Cell-Cycle Analyses

Cell-cycle analyses were performed as described (Yan et al., 2009). Briefly, BrdU (100 mg/kg body weight) was injected intraperitoneally (i.p.) into pregnant females 30 min and 16 hr prior to embryo harvest for estimation of S phase and cell-cycle exit indices, respectively. To assess S phase, we calculated proliferation index as $BrdU^+/Ki67^+$ cells where Ki67 marks all cycling cells, we calculated cell-cycle exit index as $BrdU^+Ki67^-/BrdU^+Ki67^+$, and we calculated mitotic index as $Mpm2^+/Ki67^+$ where Mpm2 marks cells in mitosis (Chenn and Walsh, 2002).

4-OHT Injections

4-OHT injections were performed as described (Badea et al., 2003). Briefly, 4-OHT (Sigma) was dissolved in ethanol at a concentration of 20 mg/ml and was stored in aliquots at −80°C. Aliquots were emulsified in five volumes of sunflower seed oil, centrifuged under vacuum to remove the ethanol, and delivered as a single i.p. injection.

Cell Soma Analysis

Motor neuron cell size measurements were performed on Z series confocal projection images of the LMC at L1–L4 levels. Area measurements were performed using the LSM5 Image Examiner software, and distribution histograms were constructed for each animal by grouping cell body cross-sectional areas into 20 μm bins. Average histograms were fit to dual Gaussian distributions using OriginPro8.5 (OriginLab). From the fitted distributions, average cross-sectional area and standard deviation (SD) of the small- and large-size MN populations were estimated. The threshold cutoff size for the small population was estimated as the average (μ) + 2 SD (σ) of the fitted small population distribution in control animals of similar age.

SUPPLEMENTAL INFORMATION

Supplemental Information includes six figures and Supplemental Experimental Procedures and can be found with this article online at doi:10.1016/j.neuron.2011.07.028.

ACKNOWLEDGMENTS

We thank Jeremy Dasen, Thomas Jessell, and Ben Novitch for antibodies, Zachary T. Bitzer for technical assistance, Goran Periz for antibody manufacture, members of the Sockanathan laboratory for discussions, and Alex Kolodkin and Ye Yan for comments on the manuscript. This work was funded by grants from the Muscular Dystrophy Association and from the NIH (NINDS RO1NS046336). All experiments involving animals were performed according to procedures approved by the Johns Hopkins IACUC review board.

Accepted: July 29, 2011
Published: September 21, 2011

REFERENCES

Agalliu, D., Takada, S., Agalliu, I., McMahon, A.P., and Jessell, T.M. (2009). Motor neurons with axial muscle projections specified by Wnt4/5 signaling. Neuron *61*, 708–720.

Arber, S., Han, B., Mendelsohn, M., Smith, M., Jessell, T.M., and Sockanathan, S. (1999). Requirement for the homeobox gene Hb9 in the consolidation of motor neuron identity. Neuron *23*, 659–674.

Arber, S., Ladle, D.R., Lin, J.H., Frank, E., and Jessell, T.M. (2000). ETS gene Er81 controls the formation of functional connections between group Ia sensory afferents and motor neurons. Cell *101*, 485–498.

Badea, T.C., Wang, Y., and Nathans, J. (2003). A noninvasive genetic/pharmacologic strategy for visualizing cell morphology and clonal relationships in the mouse. J. Neurosci. *23*, 2314–2322.

Burke, R.E., Strick, P.L., Kanda, K., Kim, C.C., and Walmsley, B. (1977). Anatomy of medial gastrocnemius and soleus motor nuclei in cat spinal cord. J. Neurophysiol. *40*, 667–680.

Buss, R.R., Gould, T.W., Ma, J., Vinsant, S., Prevette, D., Winseck, A., Toops, K.A., Hammarback, J.A., Smith, T.L., and Oppenheim, R.W. (2006). Neuromuscular development in the absence of programmed cell death: phenotypic alteration of motoneurons and muscle. J. Neurosci. *26*, 13413–13427.

Chenn, A., and Walsh, C.A. (2002). Regulation of cerebral cortical size by control of cell cycle exit in neural precursors. Science *297*, 365–369.

Corbin, J.G., Gaiano, N., Juliano, S.L., Poluch, S., Stancik, E., and Haydar, T.F. (2008). Regulation of neural progenitor cell development in the nervous system. J. Neurochem. *106*, 2272–2287.

Dasen, J.S., and Jessell, T.M. (2009). Hox networks and the origins of motor neuron diversity. Curr. Top. Dev. Biol. *88*, 169–200.

Dasen, J.S., Liu, J.P., and Jessell, T.M. (2003). Motor neuron columnar fate imposed by sequential phases of Hox-c activity. Nature *425*, 926–933.

Dasen, J.S., Tice, B.C., Brenner-Morton, S., and Jessell, T.M. (2005). A Hox regulatory network establishes motor neuron pool identity and target-muscle connectivity. Cell *123*, 477–491.

Dasen, J.S., De Camilli, A., Wang, B., Tucker, P.W., and Jessell, T.M. (2008). Hox repertoires for motor neuron diversity and connectivity gated by a single accessory factor, FoxP1. Cell *134*, 304–316.

De Marco Garcia, N.V., and Jessell, T.M. (2008). Early motor neuron pool identity and muscle nerve trajectory defined by postmitotic restrictions in Nkx6.1 activity. Neuron *57*, 217–231.

Dehay, C., and Kennedy, H. (2007). Cell-cycle control and cortical development. Nat. Rev. Neurosci. *8*, 438–450.

Diez del Corral, R., Olivera-Martinez, I., Goriely, A., Gale, E., Maden, M., and Storey, K. (2003). Opposing FGF and retinoid pathways control ventral neural pattern, neuronal differentiation, and segmentation during body axis extension. Neuron *40*, 65–79.

Fetcho, J.R. (1992). The spinal motor system in early vertebrates and some of its evolutionary changes. Brain Behav. Evol. *40*, 82–97.

Friese, A., Kaltschmidt, J.A., Ladle, D.R., Sigrist, M., Jessell, T.M., and Arber, S. (2009). Gamma and alpha motor neurons distinguished by expression of transcription factor Err3. Proc. Natl. Acad. Sci. USA *106*, 13588–13593.

Gallazzini, M., Ferraris, J.D., and Burg, M.B. (2008). GDPD5 is a glycerophosphocholine phosphodiesterase that osmotically regulates the osmoprotective organic osmolyte GPC. Proc. Natl. Acad. Sci. USA *105*, 11026–11031.

Grillner, S., and Jessell, T.M. (2009). Measured motion: searching for simplicity in spinal locomotor networks. Curr. Opin. Neurobiol. *19*, 572–586.

Gutman, C.R., Ajmera, M.K., and Hollyday, M. (1993). Organization of motor pools supplying axial muscles in the chicken. Brain Res. *609*, 129–136.

Haase, G., Dessaud, E., Garcès, A., de Bovis, B., Birling, M., Filippi, P., Schmalbruch, H., Arber, S., and deLapeyrière, O. (2002). GDNF acts through PEA3 to regulate cell body positioning and muscle innervation of specific motor neuron pools. Neuron *35*, 893–905.

Huber, A.B., Kania, A., Tran, T.S., Gu, C., De Marco Garcia, N., Lieberam, I., Johnson, D., Jessell, T.M., Ginty, D.D., and Kolodkin, A.L. (2005). Distinct roles for secreted semaphorin signaling in spinal motor axon guidance. Neuron *48*, 949–964.

Hui, K., Kucera, J., and Henderson, J.T. (2008). Differential sensitivity of skeletal and fusimotor neurons to Bcl-2-mediated apoptosis during neuromuscular development. Cell Death Differ. *15*, 691–699.

Ji, S.J., Periz, G., and Sockanathan, S. (2009). Nolz1 is induced by retinoid signals and controls motoneuron subtype identity through distinct repressor activities. Development *136*, 231–240.

Jung, H., Lacombe, J., Mazzoni, E.O., Liem, K.F., Jr., Grinstein, J., Mahony, S., Mukhopadhyay, D., Gifford, D.K., Young, R.A., Anderson, K.V., et al. (2010). Global control of motor neuron topography mediated by the repressive actions of a single hox gene. Neuron *67*, 781–796.

Kanning, K.C., Kaplan, A., and Henderson, C.E. (2010). Motor neuron diversity in development and disease. Annu. Rev. Neurosci. *33*, 409–440.

Landmesser, L. (1978). The distribution of motoneurones supplying chick hind limb muscles. J. Physiol. *284*, 371–389.

Landmesser, L.T. (2001). The acquisition of motoneuron subtype identity and motor circuit formation. Int. J. Dev. Neurosci. *19*, 175–182.

Lee, S.K., and Pfaff, S.L. (2003). Synchronization of neurogenesis and motor neuron specification by direct coupling of bHLH and homeodomain transcription factors. Neuron *38*, 731–745.

Lin, J.H., Saito, T., Anderson, D.J., Lance-Jones, C., Jessell, T.M., and Arber, S. (1998). Functionally related motor neuron pool and muscle sensory afferent subtypes defined by coordinate ETS gene expression. Cell *95*, 393–407.

Marklund, U., Hansson, E.M., Sundström, E., de Angelis, M.H., Przemeck, G.K., Lendahl, U., Muhr, J., and Ericson, J. (2010). Domain-specific control of neurogenesis achieved through patterned regulation of Notch ligand expression. Development *137*, 437–445.

Matise, M.P., and Lance-Jones, C. (1996). A critical period for the specification of motor pools in the chick lumbosacral spinal cord. Development *122*, 659–669.

Namihira, M., Kohyama, J., Semi, K., Sanosaka, T., Deneen, B., Taga, T., and Nakashima, K. (2009). Committed neuronal precursors confer astrocytic potential on residual neural precursor cells. Dev. Cell *16*, 245–255.

Nogusa, Y., Fujioka, Y., Komatsu, R., Kato, N., and Yanaka, N. (2004). Isolation and characterization of two serpentine membrane proteins containing glycerophosphodiester phosphodiesterase, GDE2 and GDE6. Gene *337*, 173–179.

Nornes, H.O., and Carry, M. (1978). Neurogenesis in spinal cord of mouse: an autoradiographic analysis. Brain Res. *159*, 1–6.

Novitch, B.G., Wichterle, H., Jessell, T.M., and Sockanathan, S. (2003). A requirement for retinoic acid-mediated transcriptional activation in ventral neural patterning and motor neuron specification. Neuron *40*, 81–95.

Peng, C.Y., Yajima, H., Burns, C.E., Zon, L.I., Sisodia, S.S., Pfaff, S.L., and Sharma, K. (2007). Notch and MAML signaling drives Scl-dependent interneuron diversity in the spinal cord. Neuron *53*, 813–827.

Prasad, A., and Hollyday, M. (1991). Development and migration of avian sympathetic preganglionic neurons. J. Comp. Neurol. *307*, 237–258.

Rao, M., and Sockanathan, S. (2005). Transmembrane protein GDE2 induces motor neuron differentiation in vivo. Science *309*, 2212–2215.

Rousso, D.L., Gaber, Z.B., Wellik, D., Morrisey, E.E., and Novitch, B.G. (2008). Coordinated actions of the forkhead protein Foxp1 and Hox proteins in the columnar organization of spinal motor neurons. Neuron *59*, 226–240.

Seuntjens, E., Nityanandam, A., Miquelajauregui, A., Debruyn, J., Stryjewska, A., Goebbels, S., Nave, K.A., Huylebroeck, D., and Tarabykin, V. (2009). Sip1 regulates sequential fate decisions by feedback signaling from postmitotic neurons to progenitors. Nat. Neurosci. *12*, 1373–1380.

Shah, V., Drill, E., and Lance-Jones, C. (2004). Ectopic expression of Hoxd10 in thoracic spinal segments induces motoneurons with a lumbosacral molecular profile and axon projections to the limb. Dev. Dyn. *231*, 43–56.

Shneider, N.A., Brown, M.N., Smith, C.A., Pickel, J., and Alvarez, F.J. (2009). Gamma motor neurons express distinct genetic markers at birth and require muscle spindle-derived GDNF for postnatal survival. Neural Dev. *4*, 42.

Thaler, J.P., Harrison, K., Sharma, K., Lettieri, K., Kehrl, J., and Pfaff, S.L. (1999). Active suppression of interneuron programs within developing motor neurons revealed by analysis of homeodomain factor HB9. Neuron *23*, 675–687.

Thaler, J.P., Lee, S.K., Jurata, L.W., Gill, G.N., and Pfaff, S.L. (2002). LIM factor Lhx3 contributes to the specification of motor neuron and interneuron identity through cell-type-specific protein-protein interactions. Cell *110*, 237–249.

Tsuchida, T.N., Ensini, M., Morton, S.B., Baldassare, M., Edlund, T., Jessell, T.M., and Pfaff, S.L. (1994). Topographic organization of embryonic motor neurons defined by expression of LIM homeobox genes. Cell *79*, 957–970.

Vrieseling, E., and Arber, S. (2006). Target-induced transcriptional control of dendritic patterning and connectivity in motor neurons by the ETS gene Pea3. Cell *127*, 1439–1452.

Whitelaw, V., and Hollyday, M. (1983). Thigh and calf discrimination in the motor innervation of the chick hindlimb following deletions of limb segments. J. Neurosci. *3*, 1199–1215.

Wu, Y., Wang, G., Scott, S.A., and Capecchi, M.R. (2008). Hoxc10 and Hoxd10 regulate mouse columnar, divisional and motor pool identity of lumbar motoneurons. Development *135*, 171–182.

Yan, Y., Sabharwal, P., Rao, M., and Sockanathan, S. (2009). The antioxidant enzyme Prdx1 controls neuronal differentiation by thiol-redox-dependent activation of GDE2. Cell *138*, 1209–1221.

Yanaka, N., Imai, Y., Kawai, E., Akatsuka, H., Wakimoto, K., Nogusa, Y., Kato, N., Chiba, H., Kotani, E., Omori, K., and Sakurai, N. (2003). Novel membrane protein containing glycerophosphodiester phosphodiesterase motif is transiently expressed during osteoblast differentiation. J. Biol. Chem. *278*, 43595–43602.

Zhuang, B., Su, Y.S., and Sockanathan, S. (2009). FARP1 promotes the dendritic growth of spinal motor neuron subtypes through transmembrane Semaphorin6A and PlexinA4 signaling. Neuron *61*, 359–372.